

Communication-Efficient and Decentralized Multi-Task Boosting while Learning the Collaboration Graph

Valentina Zantedeschi^{*1}, Aurélien Bellet^{†2}, and Marc Tommasi^{‡3}

¹Univ Lyon, UJM-Saint-Etienne, CNRS, Institut d Optique Graduate School, Laboratoire Hubert Curien UMR 5516, F-42023, SAINT-ETIENNE, France

²INRIA, France

³Université de Lille, France

Abstract

We study the decentralized machine learning scenario where many users collaborate to learn personalized models based on (i) their local datasets and (ii) a similarity graph over the users’ learning tasks. Our approach trains nonlinear classifiers in a multi-task boosting manner without exchanging personal data and with low communication costs. When background knowledge about task similarities is not available, we propose to jointly learn the personalized models and a sparse collaboration graph through an alternating optimization procedure. We analyze the convergence rate, memory consumption and communication complexity of our decentralized algorithms, and demonstrate the benefits of our approach compared to competing techniques on synthetic and real datasets.

1 Introduction

In the era of big data, the classical paradigm is to build huge data centers to collect and process users’ data. This centralized access to resources and datasets simplifies some procedures, such as building predictive models with machine learning, but also comes with important drawbacks. From the company point of view, the need to gather and analyze the data centrally induces high infrastructure costs. As the server represents a single point of entry, it must also be secure enough to prevent attacks that could put the entire user database in jeopardy. On the user end, disadvantages include limited control over one’s personal data as well as possible privacy risks, which may come from the aforementioned attacks but also from potentially loose data governance policies on the part of the companies. A more subtle risk is to be trapped in a “single thought” model which fades individual users’ specificities or leads to unfair predictions for some of the users.

For all these reasons and thanks to the advent of powerful personal devices, we are currently witnessing a shift to a more decentralized paradigm. In the context of machine learning, this shift translates into keeping the data on the users’ devices and leveraging their resources to train the predictive models in a collaborative manner. This requires to drop a key assumption of traditional distributed learning approaches (Bekkerman et al., 2011; Zhang et al., 2012, 2013; Shamir and Srebro, 2014; Arjevani and Shamir, 2015; Ma et al., 2017), namely that the data is balanced and uniformly distributed across machines. There are two main lines of work in this direction. In federated learning (McMahan et al., 2017; Konečný et al., 2016a,b), each client computes an update of the current global model based on its local data and sends it to a coordinator, which aggregates the updates and broadcasts the result back to the clients. In practice, the dependence on the

^{*}first.last@univ-st-etienne.fr

[†]first.last@inria.fr

[‡]first.last@inria.fr

coordinator creates a single point of failure as well as a communication bottleneck when the number of clients is large (Lian et al., 2017). Decentralized learning aims to fix this problem by relying only on local peer-to-peer exchanges in a sparse communication graph (Nedic and Ozdaglar, 2009; Duchi et al., 2012; Wei and Ozdaglar, 2012; Colin et al., 2016; Lian et al., 2017; Tang et al., 2018b). In both federated and decentralized learning, low communication is key to the efficiency of the algorithms, motivating strategies to reduce the communication complexity while preserving good accuracy (Zhang et al., 2012; Konečný et al., 2016b; Suresh et al., 2017; Tang et al., 2018a).

Another promising and complementary direction to further account for differences in the users' datasets is to learn personalized models in a multi-task fashion instead of assuming that there exists a single model which is accurate for everyone. The hope is to improve the user experience by modeling its specific taste and data distribution. This has been recently explored in both federated (Smith et al., 2017) and decentralized settings (Vanhaesebrouck et al., 2017; Bellet et al., 2018) by regularizing personal models to be close for "similar" users so as to improve generalization. Unfortunately, designing appropriate similarity scores is often challenging, especially in the decentralized scenario. The above approaches are further restricted to linear models, and it is not clear how to extend them to nonlinear models while retaining their convergence guarantees.

In this paper, we propose a decentralized method for collaboratively learning personalized nonlinear classifiers with low communication cost. We first introduce a novel formulation based on l_1 -Adaboost (Shen and Li, 2010), which allows to build nonlinear classifiers as combinations of a set of base predictors. We achieve collaboration and personalization by introducing a trade-off between (i) making the personal model of a user accurate on its local dataset, and (ii) selecting base classifiers that are popular among the user's neighbors in a fixed collaboration graph describing task relationships. We propose a Frank-Wolfe algorithm (Frank and Wolfe, 1956) to solve the problem in the decentralized setting, where the collaboration graph is seen as an overlay over a physical communication network. At each iteration, a randomly selected user greedily updates its personal model by incorporating a single base predictor at a time and sends the update to its direct neighbors in the graph. These sparse updates allow for very low communication costs (logarithmic in the number of base classifiers to combine). Our last contribution is a decentralized algorithm for learning the collaboration graph along with the personalized classifiers in an alternating optimization fashion. The proposed graph learning strategy can be used in conjunction with any loss function and allows to easily tune the graph sparsity. Combined with our decentralized boosting algorithm, we can therefore control the overall communication costs through sparse updates and reduced neighborhoods. We analyze the convergence rate, memory consumption and communication complexity of our algorithms and empirically compare their performance to state-of-the-art decentralized techniques.

The main advantages of our approach with respect to previous work on collaborative personalized learning (Smith et al., 2017; Vanhaesebrouck et al., 2017; Bellet et al., 2018) are: (i) We learn *nonlinear* classifiers by modeling the multi-task problem as graph-regularized boosting. (ii) We design a decentralized training algorithm that operates under *very low communication costs*. (iii) We *jointly learn the sparse collaboration graph* when it is not available.

The rest of the paper is organized as follows. Section 2 introduces some notations and our collaborative personalized boosting formulation. In Section 3, we describe and analyze our decentralized algorithm to learn the classifiers given the collaboration graph. Section 4 extends the previous framework by allowing to learn the collaboration graph together with the classifiers. Section 5 discusses some related work, and some experiments are presented in Section 6. Finally, we discuss promising future directions in Section 7.

2 Collaborative Personalized Boosting

Setup and notations. We consider a set of learning agents (users) $[K] = \{1, \dots, K\}$, each with a personal binary classification task over a common feature space \mathcal{X} . Agent k holds a local dataset S_k of m_k labeled examples drawn from its personal data distribution over $\mathcal{X} \times \{-1, 1\}$. For example, each personal task could be to predict whether the agent likes a given item based on features describing the item. We denote by $m = \sum_{k=1}^K m_k$ the total number of samples and by $S = \bigcup_{k=1}^K S_k = \{(x_i, y_i)\}_{i=1}^m$ the union of the local datasets where observations $x_i \in \mathcal{X}$ are associated with a label $y_i \in \{-1, 1\}$. As agents have datasets of different sizes,

we introduce a “confidence” value $c_k \in \mathbb{R}^+$ for each agent k which should be thought of as proportional to m_k . In practice, we simply set $c_k = \frac{m_k}{\max_i m_i}$.

We will work with a set of n real-valued base predictors $H = \{h_j : \mathcal{X} \rightarrow \mathbb{R}\}_{j=1}^n$. These can be for instance weak classifiers (e.g., decision stumps) as in standard boosting, or stronger predictors that were pre-trained on separate data (e.g., public, crowdsourced, or collected from users who opted in to share personal data). Each agent k aims at learning a binary classifier in the form of a linear combination of the base predictors in H , i.e. a mapping $x \mapsto \text{sign}[\sum_{j=1}^n [\alpha_k]_j h_j(x)]$ parameterized by a weight vector $\alpha_k \in \mathbb{R}^n$. We will denote by $A \in \mathbb{R}^{m \times n}$ the matrix whose entry $a_{ij} = y_i h_j(x_i)$ gives the margin achieved by the base classifier $h_j \in H$ on the training sample $(x_i, y_i) \in S$. We will also use $A_k \in \mathbb{R}^{m_k \times n}$ to denote the margin matrix restricted to the samples in the dataset S_k of agent k , so that for $i \in [m_k]$, $[A_k \alpha_k]_i = y_i \sum_{j=1}^n [\alpha_k]_j h_j(x_i)$ gives the margin achieved by the classifier α_k on the i -th data point in S_k . Only agent k is assumed to have access to A_k .

Instead of learning the model of each agent independently, we consider a collaborative multi-task setting where agents leverage an undirected and weighted collaboration graph $\mathcal{G} = ([K], E, w)$ to learn better classifiers. Each edge weight $w_{k,l} \geq 0$ is assumed to reflect the similarity between the learning tasks of agents k and l , with $w_{k,l} = 0$ for $(k, l) \notin E$. For notational convenience, we store the weights in a vector $w = (w_{k,l})_{k,l \in [K], k < l}$ of dimension $K(K-1)/2$. We denote by $d_k = \sum_{l=1}^K w_{k,l}$ the degree of node k and by $d = (d_1, \dots, d_K) \in \mathbb{R}^K$ the degree vector. For now, we assume this collaboration graph to be given as input to the algorithm. In Section 4, we will propose an approach to learn it together with the classifiers.

Objective function. We now introduce a joint optimization problem over the classifiers $\alpha = [\alpha_1, \dots, \alpha_K] \in (\mathbb{R}^n)^K$. It is essentially a multi-task version of l_1 -Adaboost (Shen and Li, 2010) with additional graph regularization:

$$\min_{\alpha \in \mathcal{M}} \sum_{k=1}^K d_k c_k \log\left(\sum_{i=1}^{m_k} e^{-[A_k \alpha_k]_i}\right) + \frac{\mu}{2} \sum_{k < l} w_{k,l} \|\alpha_k - \alpha_l\|^2, \quad (1)$$

where $\mathcal{M} = \{\alpha \in (\mathbb{R}^n)^K : \forall i, \|\alpha_i\|_1 \leq \beta\}$. The objective function in (1), which we will denote by $f(\alpha)$, is composed of two terms. The first one is a sum of Adaboost logistic loss functions (one per agent), involving only their personal model and local dataset. The parameter β bounds the l_1 norm of the learned models to encourage sparsity. The second term is a graph regularization term that enables collaboration by encouraging each agent k to select the same weak classifiers as another agent l in the collaboration graph if the edge weight $w_{k,l}$ is large (d_k in the loss term prevents the objective from being sensitive to the absolute scale of graph weights). Notice that the confidence c_k in the first term adjusts the trade-off between these two terms differently for each agent depending on how much local data the agent holds. The parameter μ is used to globally balance the two terms. The case $\mu = 0$ corresponds to having each agent k learn its classifier α_k in isolation by minimizing the loss on its local dataset. On the other hand, as $\mu \rightarrow +\infty$ the problem reduces to learning a single global model that minimizes the sum of all local losses. The objective function is convex and continuously differentiable, and the feasible domain is a compact and convex subset of $(\mathbb{R}^n)^K$.

3 Decentralized Collaborative Boosting of Personalized Models

3.1 Decentralized Frank-Wolfe Algorithm

In this section, we propose an approach to solve Problem (1) in the decentralized setting. Our algorithm is based on Frank-Wolfe (FW) (Frank and Wolfe, 1956; Jaggi, 2013), which has recently been proposed to solve l_1 -Adaboost in the centralized and non-personalized setting (Wang et al., 2015). For clarity of presentation, we set aside the decentralized setting for now and derive the Frank-Wolfe update for the model of an agent according to our formulation (1).

FW update. The main idea of FW is to iteratively update the current solution by moving towards the minimizer of the linearized objective over the feasible domain. Let us denote by $\alpha^{(t-1)} \in \mathcal{M}$ the current models at time step $t-1$. Applied to problem (1) and restricting our attention to the model of agent k , a FW update takes the form $\alpha_k^{(t)} = (1 - \gamma)\alpha_k^{(t-1)} + \gamma s_k^{(t)}$ with $\gamma \in [0, 1]$ the step size,

$$s_k^{(t)} = \arg \min_{\|s\|_1 \leq \beta} s^\top g_k^{(t)}, \quad (2)$$

and $g_k^{(t)} = \nabla[f(\alpha^{(t-1)})]_k \in \mathbb{R}^n$ the partial derivative of f with respect to the k -th block of coordinates (corresponding to the model of agent k). Note incidentally that the FW update takes the form of a convex combination of two feasible points, hence the updated model remains feasible (i.e., we have $\|\alpha_k^{(t)}\|_1 \leq \beta$).

As shown in (Clarkson, 2010; Jaggi, 2013), a solution to (2) is given by $\beta \text{sign}(-(g_k^{(t)})_{j_k^{(t)}}) \mathbf{e}^{j_k^{(t)}}$ where $j_k^{(t)} = \arg \max_j [|g_k^{(t)}|]_j$ and $\mathbf{e}^{j_k^{(t)}}$ is the unit vector with 1 in the $j_k^{(t)}$ -th entry. In other words, FW updates a single coordinate of the current model $\alpha_k^{(t-1)}$ which corresponds to the maximum absolute value entry of the partial gradient $g_k^{(t)}$. For Problem (1), the partial gradient is given by

$$g_k^{(t)} = -d_k c_k \eta_k^\top A_k + \mu(d_k \alpha_k^{(t-1)} - \sum_l w_{k,l} \alpha_l^{(t-1)}),$$

with $\eta_k = \frac{\exp(-A_k \alpha_k^{(t-1)})}{\sum_{i=1}^{m_k} \exp(-A_k \alpha_k^{(t-1)})_i}$. The first term in $g_k^{(t)}$ plays the same role as in standard Adaboost: the j -th entry (corresponding to the base predictor h_j) is larger when h_j achieves a large margin on the training sample S_k reweighted by η_k (i.e., points that are currently poorly classified get more importance). On the other hand, the more h_j is used by the neighbors of k , the larger the j -th entry of the second term. By applying the FW update (2), we are, thus, able to keep the flavor of boosting (incorporating a single base classifier at a time which performs well on the reweighted sample) with an additional bias towards selecting base predictors that are popular amongst neighbors. The relative importance of the two terms depends on the agent confidence c_k .

Decentralized algorithm. Building upon these ideas, we now propose a FW algorithm to solve Problem (1) in the decentralized setting. Each agent corresponds to a machine in a physical network, and keeps its personal dataset locally. The collaboration graph $\mathcal{G} = ([K], E, w)$ defined in Section 2 plays the role of an overlay network that allows agent k to communicate with its direct neighbors $N_k = \{l : (k, l) \in E\}$ in \mathcal{G} . $|N_k|$ will typically be much smaller than K so that updates can occur in parallel in different parts of the network, ensuring that the procedure scales well with the number of users. As standard in the literature of decentralized algorithms (see e.g., Boyd et al., 2006), we consider that each agent k is equipped with a local clock ticking independently following a 1-Poisson distribution. Equivalently, one can consider a global clock (with counter t) which ticks each time one of the local clock ticks. When the local clock of agent k ticks, the agent wakes up to update its personal classifier α_k and then broadcasts the update to its neighborhood N_k .

More formally, our algorithm proceeds as follows. Each personal classifier $\alpha_k^{(0)}$ is initialized to some feasible point (such as the zero vector). Then, at each step $t \geq 1$, a random agent k wakes up and performs the following actions:

1. *Update step:* agent k performs a Frank-Wolfe update on its local model based on the most recent information $\alpha_l^{(t-1)}$ received from its neighbors $l \in N_k$:

$$\alpha_k^{(t)} = (1 - \gamma^{(t)}) \alpha_k^{(t-1)} + \gamma^{(t)} s_k^{(t)},$$

where $s_k^{(t)} = \beta \text{sign}(-(g_k^{(t)})_{j_k^{(t)}}) \mathbf{e}^{j_k^{(t)}}$, $\gamma^{(t)} = \frac{2K}{t+2K}$.

2. *Communication step:* agent k sends its updated model $\alpha_k^{(t)}$ to its neighborhood N_k .

The other models remain unchanged. The update step corresponds to a block coordinate Frank-Wolfe step (Lacoste-Julien et al., 2013) and only requires the knowledge of the models of neighboring agents, which were received at earlier iterations. Thanks to the sparsity of the FW updates, we will see in Section 3.3 that the communication step can be performed at very low cost.

3.2 Convergence Analysis

The convergence analysis of our algorithm follows the proof technique proposed by Jaggi (2013) and refined by Lacoste-Julien et al. (2013) for the case of block coordinate Frank-Wolfe. The analysis is based on defining

an appropriate surrogate for the optimality gap $f(\alpha) - f(\alpha^*)$, where α^* is a solution to Problem (1). Under an appropriate notion of smoothness of f over the feasible domain \mathcal{M} , the convergence of Frank-Wolfe is established by showing that the gap decreases in expectation with the number of iterations, because at a given iteration t the block-wise surrogate gap at the current solution is minimized by the greedy update $s_k^{(t)}$. The following result shows an $O(1/t)$ convergence rate (see supplementary material for the proof).

Theorem 1. *Our decentralized Frank-Wolfe algorithm takes at most $6K(C_f^\otimes + p_0)/\varepsilon$ iterations to find an approximate solution α that satisfies, in expectation, $f(\alpha) - f(\alpha^*) \leq \varepsilon$, where $C_f^\otimes \leq 4\beta^2 \sum_{k=1}^K (d_k c_k \|A_k\|_1^2 + \mu d_k)$ and $p_0 = f(\alpha^{(0)}) - f(\alpha^*)$ is the initial sub-optimality gap.*

3.3 Communication and Memory Cost

We study the communication and memory costs of our algorithm for a generic collaboration graph $\mathcal{G} = ([K], E, w)$ with K nodes and M edges. Recall that the number of base predictors to combine is denoted by n . The following analysis stands for systems without failure (all sent messages are correctly received). We express all costs in number of bits, and Z denotes the bit length used to represent floats.

Memory. Each agent needs to store its current model, a copy of its neighbors' models, and the similarity weights associated with its neighbors. Denoting by $|N_k|$ the number of neighbors of agent k , its memory cost is given by $Z(n + |N_k|(n + 1))$, which leads to a total cost for the network of

$$KZ(n + \sum_{k=1}^K |N_k|(n + 1)) = Z(Kn + 2M(n + 1)).$$

The total memory is thus linear in M , K and n . Thanks to the sparsity of the updates, the dependency on n can be reduced from linear to logarithmic by representing models as sparse vectors. Specifically, when initializing the models to zero vectors, the model of an agent k who has performed t_k updates so far contains at most t_k nonzero elements and can be represented using $t_k(Z + \log n)$ bits: t_kZ for the nonzero values and $t_k \log n$ for their indices.

Communication. At each iteration, an agent k updates a single coordinate of its model α_k . Hence, it is enough to send to the neighbors the index of the modified coordinate and its new value (or the index and the step size $\gamma_k^{(t)}$). Therefore, the communication cost of a single iteration is equal to $(Z + \log n)|N_k|$. This is in contrast to previous federated/decentralized approaches for learning personalized models (Smith et al., 2017; Vanhaesebrouck et al., 2017; Bellet et al., 2018), whose communication cost scales linearly with the number of parameters of the model (which corresponds to the data dimension). After T iterations, the expected total communication cost for our approach is

$$T(Z + \log n)\mathbb{E}_{k \sim \mathcal{U}(1, K)}[|N_k|] = 2TMK^{-1}(Z + \log n).$$

Combining this with Theorem 1, the communication cost needed to obtain an optimization error smaller than ε amounts to $\frac{12M(C_f + h_0)}{\varepsilon}(Z + \log n)$.

4 Learning the Collaboration Graph

Until now, we have assumed that the collaboration graph $\mathcal{G} = ([K], E, w)$ describing the affinities between agents was given. In practical applications, the graph weights w may be computed based on side information on the agents (e.g., user profiles), but this is not always available or reliable. Instead, we propose to jointly optimize an extended version of our problem (1) over α and w .

4.1 General Formulation

To emphasize the generality of our contribution, we will work with arbitrary model families and loss functions: we simply denote by $\mathcal{L}_k(\alpha_k; S_k)$ the loss function of agent k on its local dataset S_k . \mathcal{L}_k may for instance be the Adaboost logistic loss function introduced in Section 2.

We now introduce our joint formulation for learning the personalized models and the collaboration graph:

$$\min_{\substack{\alpha \in \mathcal{M} \\ w \in \mathcal{W}}} \sum_{k=1}^K d_k c_k \mathcal{L}_k(\alpha_k; S_k) + \mu \left(\frac{1}{2} \sum_{k < l} w_{k,l} \|\alpha_k - \alpha_l\|^2 - \mathbf{1}^\top \log(d + \delta) + \lambda \|w\|^2 \right), \quad (3)$$

where $\mathcal{W} = \{w \in \mathbb{R}^{K(K-1)/2} : w \geq 0\}$ and $d = (d_1, \dots, d_K)$ is the vector of node degrees ($d_k = \sum_{l=1}^K w_{k,l}$). The last two terms are inspired by the graph learning formulation of Kalofolias (2016). The log term ensures that all nodes have nonzero degrees. The small positive constant δ is a simple trick to make the logarithm smooth on the feasible domain (see e.g., Koriche, 2018), which will make the objective easier to optimize in the decentralized setting. Most importantly, the hyperparameter $\lambda > 0$ provides a direct way to tune the sparsity of the graph (the smaller, the sparser) and hence the amount of collaboration.¹ This will allow us to control the trade-off between accuracy and communication (see the analysis of Section 3.3 and the experiments of Section 6). Finally, note that the first term penalizes large degrees more for agents with large loss values (weighted by the confidence). This implements a desirable inductive bias: it avoids connecting an agent strongly if it damages too much its local loss, unless it has low confidence (in this case, local data is scarce and one should rely more on information from other agents).

Problem (3) is not jointly convex in w and α , but it is bi-convex. It is thus natural to solve it by alternating minimization on the models $\alpha = [\alpha_1, \dots, \alpha_K]$ and the graph weights w . To optimize the models given the graph, one can readily use the decentralized algorithm introduced in Section 3, or those of Vanhaesebrouck et al. (2017) and Bellet et al. (2018) for learning linear models. In the rest of this section, we design a decentralized algorithm to solve the graph learning subproblem (optimize w given the models α). We denote the corresponding objective function by $h(w)$.

4.2 Decentralized Graph Learning

Kalofolias (2016) describes a centralized primal-dual algorithm for a related graph learning problem, which requires global knowledge of all graph weights and pairwise distances between models. In contrast, our goal is to design a decentralized algorithm allowing each agent to update its weights asynchronously and in parallel based on a local view of the network. We will rely on the availability of a peer sampling service (Jelasity et al., 2007), a classic distributed systems primitive allowing an agent to communicate with a random set of other agents (peers) in the network.

More formally, let $\kappa \in \{1, \dots, K-1\}$ be a fixed parameter of the algorithm. At each step, a random agent k wakes up and samples uniformly and without replacement a set \mathcal{K} of κ agents from the set $\{1, \dots, K\} \setminus \{k\}$ using the peer sampling service. For convenience, for a vector $w \in \mathbb{R}^{K(K-1)/2}$ we will denote by $w_{k,\mathcal{K}}$ its κ -dimensional subvector corresponding to the entries $\{(k, l)\}_{l \in \mathcal{K}}$. We denote by $\Delta_{k,\mathcal{K}} = (\|\alpha_k - \alpha_l\|^2)_{l \in \mathcal{K}}$ the vector of distances between the model of agent k and those of agents in \mathcal{K} , and we let $p_{k,\mathcal{K}} = (c_k \mathcal{L}_k(\alpha_k; S_k) + c_l \mathcal{L}_l(\alpha_l; S_l))_{l \in \mathcal{K}}$ and $v_{k,\mathcal{K}} = (\frac{1}{d_k + \delta} + \frac{1}{d_l + \delta})_{l \in \mathcal{K}}$. Equipped with these notations, the partial derivative of the objective function $h(w)$ with respect to the variables $w_{k,\mathcal{K}}$ can be written as follows:

$$[\nabla h(w)]_{k,\mathcal{K}} = p_{k,\mathcal{K}} + \mu \left(\frac{1}{2} \Delta_{k,\mathcal{K}} - v_{k,\mathcal{K}} + 2\lambda w_{k,\mathcal{K}} \right). \quad (4)$$

Crucially, agent k only needs to know the current degree, the loss value and the model of agents in \mathcal{K} to compute (4).

We can now state the algorithm. We start from some initial weight vector $w^{(0)} \in \mathcal{W}$. At each time step t , a random agent k wakes up and performs the following actions:

1. Draw a set \mathcal{K} of κ agents and request their current models and degree.
2. Update the associated weights:

$$w_{k,\mathcal{K}}^{(t+1)} \leftarrow \max \left(0, w_{k,\mathcal{K}}^{(t)} - \frac{1}{L_\kappa} [\nabla h(w^{(t)})]_{k,\mathcal{K}} \right), \quad (5)$$

¹We do not use a hyperparameter on the log-degree term as this has simply a scaling effect on the weights, see Kalofolias (2016).

where $L_\kappa = 2\mu(\frac{\kappa+1}{\delta^2} + \lambda)$ is the block Lipschitz constant of ∇h (see supplementary material for details).

3. Send each updated weight $w_{k,l}^{(t+1)}$ to the associated agent in $l \in \mathcal{K}$.

The algorithm is fully decentralized: no global information is needed by an agent to update its weights (local information from agents in \mathcal{K} is sufficient). Updates can thus happen asynchronously and in parallel. The step size $1/L_\kappa$, given by the Lipschitz constant, is often quite conservative: in practice we tune this step size to speed up convergence.

Remark 1 (Reducing the number of variables). *To reduce the number of variables to optimize, each agent can keep to 0 the weights corresponding to users whose current model is most different to theirs. This heuristic has a negligible impact on the solution quality in sparse regimes (small λ).*

4.3 Convergence Analysis

At a high level, our analysis proceeds as follows. We first show that our algorithm can be seen as an instance of proximal coordinate descent (PCD) (Richtárik and Takáć, 2014) on a slightly modified objective function. Unlike the standard PCD setting which focuses on disjoint blocks, our coordinate blocks exhibit a specific overlapping structure that arises as soon as $\kappa > 1$ (this is due to the fact that each weight is shared by two agents). We then build upon the PCD analysis due to Wright (2015), which we adapt to account for our overlapping block structure. The details of our analysis and the computation of strong convexity and smoothness parameters can be found in the supplementary material. We obtain the following result.

Theorem 2. *Let $T > 0$ and h^* be the optimal objective value. Our algorithm cuts the expected suboptimality gap by a constant factor ρ at each iteration: we have $\mathbb{E}[h(w^{(T)}) - h^*] \leq \rho^T (h(w^{(0)}) - h^*)$ where ρ is given by*

$$\rho = 1 - \frac{2}{K(K-1)} \frac{\kappa\lambda\delta^2}{\kappa + 1 + \lambda\delta^2}. \quad (6)$$

The linear convergence rate of Theorem 2 is typically faster than the sublinear rate of the boosting subproblem (Theorem 1), suggesting that a small number of updates per agent is sufficient to reach reasonable optimization error before re-updating the models given the new graph.

4.4 Communication vs. Convergence

At each iteration, the active agent needs to request from each agent $l \in \mathcal{K}$ its current degree d_l , its personal model $\alpha_l^{(t_\alpha)}$ and the value of its local loss, where t_α is the total number of FW model updates done so far in the network. It then sends the updated weight to each agent in \mathcal{K} . As the expected number of nonzero entries in the model of an agent is at most $\min(t_\alpha/K, n)$, the expected communication cost for a single iteration is equal to $\kappa(3Z + \min(\frac{t_\alpha}{K}, n)(Z + \log n))$, where Z is the representation length of a float. This can be further optimized if agents have enough local memory to store the models and local losses of all the agents they communicate with, as analyzed in the supplementary material.

The parameter κ can be used to trade-off the convergence speed and the amount of communication needed at each iteration, in particular when the number of agents K is large. While increasing κ results in a linear increase in the per-iteration communication cost (as well as in the number of agents to communicate with), inspecting (6) shows that the impact on ρ is mild and fades rather quickly.² This suggests that choosing $\kappa = 1$ will minimize the total communication cost needed to reach solutions of moderate precision (which is usually sufficient for machine learning). Slightly larger values (but still much smaller than K) will provide a better balance between the communication cost and the number of rounds. On the other hand, if high precision solutions are needed or if the number of communication rounds is the primary concern, large values of κ could be used. As shown in the supplementary material, the numerical behavior of our algorithm is in line with this theoretical analysis.

²This is due to the block smoothness parameter L_κ of our objective function, see supplementary material for details.

5 Related Work

In this section, we discuss in more details the two lines of previous work that are most closely related to our approach.

Distributed Boosting. Boosting methods such as Adaboost (Freund and Schapire, 1996, 1997) are principled and powerful way to construct a nonlinear classifier by adaptively combining base predictors. Several distributed versions of Adaboost have been proposed to tackle the setting where data is partitioned across a set of machines (Lazarevic and Obradovic, 2001; Wang and Zhang, 2005; Cooper and Reyzin, 2017). There has also been some work on distributed Frank-Wolfe algorithms which can be used to solve the l_1 -Adaboost problem (Bellet et al., 2015; Lafond et al., 2016). However, all the above approaches learn a single global classifier while we focus on learning personalized models.

Song et al. (2013) propose a personalized boosting approach for activity classification in microblogs. The network graph is given by a social network, and the model of each user is regularized to make similar predictions to that of its neighbors. Their approach has several drawbacks compared to ours. First, agents need to share their personal dataset with their neighbors, which is costly in terms of communication and may be undesirable due to privacy concerns. Second, the convergence of their procedure is only to a local optimum, without an established rate. Finally, they assume that the collaboration graph (social network) is known a priori.

Distributed Multi-Task Learning (MTL). Distributed MTL has been considered in (Wang et al., 2016b,a; Baytas et al., 2016; Li et al., 2017), but they typically consider a small number of tasks with well-balanced data across tasks and focus on learning linear models. Closer to our setting, recent work on federated and decentralized learning has demonstrated how fostering model smoothness for similar tasks increases the generalization performance in the presence of dataset imbalance across tasks. The federated learning approach of Smith et al. (2017) learns personalized linear models as well as similarities amongst tasks by alternating between a local step where agents optimize their own model given the task similarities, and an task similarity update performed by a central server which needs access to all current personalized models. Note that the resulting task similarities do not form a valid graph and are typically not sparse. Also focusing on linear models, Vanhaesebrouck et al. (2017) and Bellet et al. (2018) operate in the decentralized setting and propose algorithms that only rely on local communication and hence can scale to many agents. The high-level idea is to alternate between local model updates and weighted model averaging with neighbors. They however assume that the collaboration graph is given.

All these approaches have a communication cost per iteration which scales linearly with the size of model parameters (i.e., the data dimension in the case of linear models). In contrast, our approach is able to learn nonlinear models which can capture complex structure in the data while also learning a sparse collaboration graph and maintaining low communication costs. We believe that this combination of features greatly improves the applicability of the framework.

6 Experiments

In this section we study the practical behavior of our method (**Dada**, for Decentralized Adaboost) on synthetic and real-world datasets. We compare it to the following competitors, which learn either global or personalized models in a centralized or decentralized manner. **Global-Adaboost** learns a single global l_1 -Adaboost model over the centralized dataset S . **Local-Adaboost** learns a purely local personalized l_1 -Adaboost model for each agent without collaboration. Finally, **Perso-linear** is a decentralized method for collaboratively learning personalized linear models (Vanhaesebrouck et al., 2017). This approach also relies on graph regularization and can directly benefit from the decentralized graph learning approach we proposed in Section 4. We use **Dada-Learned** and **Perso-linear-Learned** when the graph is learned with our approach, and **Dada-Fixed** and **Perso-linear-Fixed** when using a pre-defined (fixed) graph. We use the same set of base predictors for all boosting-based methods (including **Dada**), namely n simple decision stumps uniformly split between all D dimensions and value ranges. We tune the following hyper-parameters with 3-fold cross validation on the training agent datasets: $\beta \in \{1, \dots, 10^3\}$ (l_1 constraint for all methods except **Perso-**

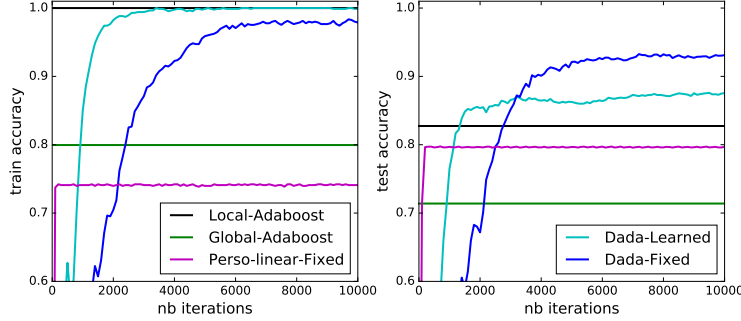


Figure 1: Training and test accuracy w.r.t. iterations on **Moons**.

linear), $\mu \in \{10^{-3}, \dots, 10^3\}$ (trade-off parameter for **Dada** and **Perso-linear**, and $\lambda \in \{10^{-3}, \dots, 10^3\}$ (graph sparsity in **Dada-Learned** and **Perso-linear-Learned**)). Models are initialized to zero vectors and the initial graphs of **Dada-Learned** and **Perso-linear-Learned** are optimized using the local classifiers obtained with **Local-Adaboost**. All accuracies are averaged over agents (see supplementary material for more results). The source code is available at <https://github.com/vzantedeschi/Dada>.

6.1 Synthetic Dataset

To study the behavior of our approach in a controlled setting, our first set of experiments is carried out on a synthetic problem (**Moons**) constructed from the classic two interleaving Moons dataset which has nonlinear class boundaries. We consider $K = 100$ agents, clustered in 4 groups of respectively $K_{c_1} = 10$, $K_{c_2} = 20$, $K_{c_3} = 30$ and $K_{c_4} = 40$ agents. Each cluster is associated with a rotation angle Θ_c of 45, 135, 225 and 315 degrees respectively. We generate a local dataset for each agent k by drawing $m_k \sim \mathcal{U}(3, 15)$ training examples and 100 test examples from the two Moons distribution. We then apply a rotation (coplanar to the Moons' distribution) to all the points according to an angle $\theta_k \sim \mathcal{N}(\Theta_c, 5)$ where c is the cluster the agent belongs to. This construction allows us to control the similarity between users (agents from the same cluster are more similar to each other than to those from different clusters). We build a “ground-truth” collaboration graph by setting $w_{k,l} = \exp\left(\frac{\cos(\theta_k - \theta_l) - 1}{\sigma}\right)$ with $\sigma = 0.1$ and dropping all edges with negligible weights, which we will give as input to **Dada-Fixed** and **Perso-linear-Fixed**. In order to increase the difficulty of the classification problems, we further add random label noise to the generated local samples by flipping the labels of 5% of the training data, and embed all points in \mathbb{R}^D space by adding random values for the $D - 2$ empty axes. In the experiments, we set $D = 20$ and the number of base predictors n to 200. For **Dada-Learned** and **Perso-linear-Learned**, the graph is updated after every 2000 iterations of optimizing α , with $\kappa = 10$ and a maximal number of iterations equal to 10^3 (see supplementary material for an empirical study of the impact of κ). The graph optimization is stopped earlier if the relative improvement of the objective function is smaller than 10^{-6} .

Learning performance. Figure 1 shows the training and test accuracy across iterations. As various optimization algorithms can be used for **Global-Adaboost** and **Local-Adaboost**, we simply display their performance at the optimal solution with a straight horizontal line. The results shows the clear gain in accuracy provided by our method. Both **Dada-Fixed** and **Dada-Learned** are successful in reducing the overfitting of **Local-Adaboost**, and achieve higher test accuracy than both **Global-Adaboost** and **Perso-linear-Fixed**. As expected, **Dada-Fixed** outperforms **Dada-Learned** as it makes use of the ground-truth graph. Despite the noise introduced by the perturbations of the angle and labels as well as by the finite sample setting, **Dada-Learned** effectively makes up for not knowing the ground-truth similarities between agents. It also allows faster accuracy improvements in earlier iterations, probably thanks to better alignment between the current graph and the current models across time. Figure 2 (left) confirms that the graph learned by **Dada-Learned** is able to approximately recover the ground-truth cluster structure. Figure 2

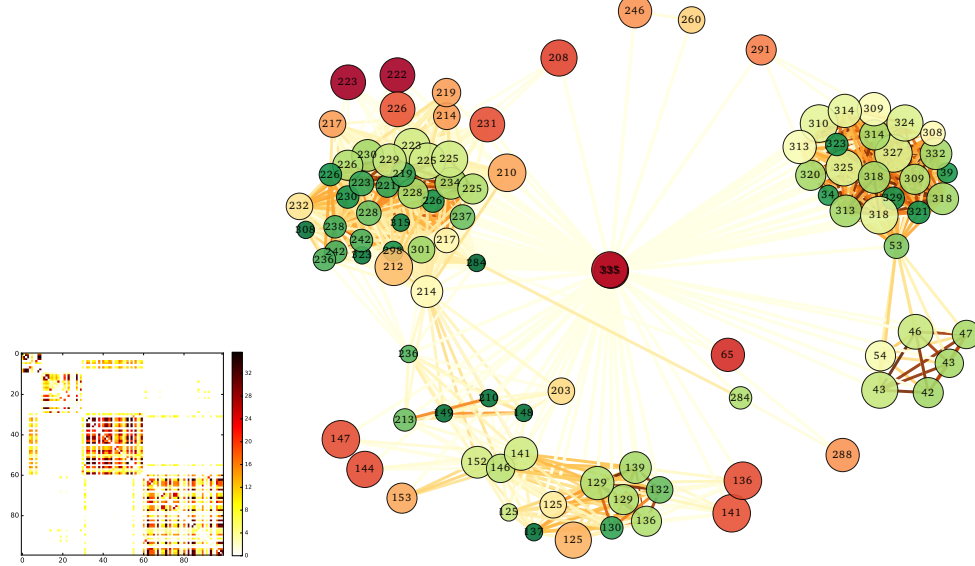


Figure 2: Graph learned on **Moons**. *Left:* Graph weights with agents ordered by their cluster membership. *Right:* Visualization of the graph. The node size is proportional to the confidence c_k and the color reflects the relative value of the local loss (greener = smaller loss). Nodes are labeled with their rotation angle, and a darker edge color indicates a higher weight.

(right) provides a more detailed visualization of the learned graph. We can clearly see the effect of the inductive bias brought by the confidence-weighted loss term in Problem (3) discussed in Section 4.1. In particular, nodes with high confidence and high loss values tend to have small degrees while nodes with low confidence or low loss values are typically more densely connected.

Communication. We now study the communication complexity of our approach. Figure 3 (left) shows the test accuracy with respect to the communication cost. We can see that **Dada** quickly reaches high accuracy. Due to the low dimensionality of this dataset ($D = 20$), the communication cost is a bit higher than for **Perso-linear-Fixed** (which has poor accuracy). **Dada** will start to outperform **Perso-linear-Fixed** in terms of communication as the dimension gets higher (see e.g., Section 6.2). Figure 3 (right) shows that the graph learned by **Dada-Learned** remains sparse across time (always sparser than the ground-truth), which ensures a small communication cost for the model update steps. On this dataset, we found that the learned graph is very stable w.r.t. the graph sparsity parameter λ , which is consistent with the underlying well-separated cluster structure. In the supplementary material, we provide experiments on a variant of this dataset without cluster structure and show that λ allows to easily tune the sparsity of the graph.

6.2 Human Activity Recognition with Smartphones

We now present some results on the real dataset **HARWS** (Anguita et al., 2013), which is composed of records from $K = 30$ users whose activities, such as walking and sitting, were captured by their smartphones' sensors. We focus on the task of distinguishing when a user is walking downstairs or upstairs, and split the associated records into 236 records for training (between 3 and 12 depending on the agent) and 2714 records for testing (between 69 and 115). Each record is described by $D = 561$ features and we set the number of stumps for the boosting-based methods to $n = 1122$. When learning the graph over this small number of agents, we update it every 200 updates of the classifiers only, and we set $\kappa = 5$ and the maximum number of iterations to 100. Note that the relationships between agents are not known for this dataset. Figure 4 shows the prediction performance of **Dada** and its competitors. **Global-Adaboost** clearly fails to

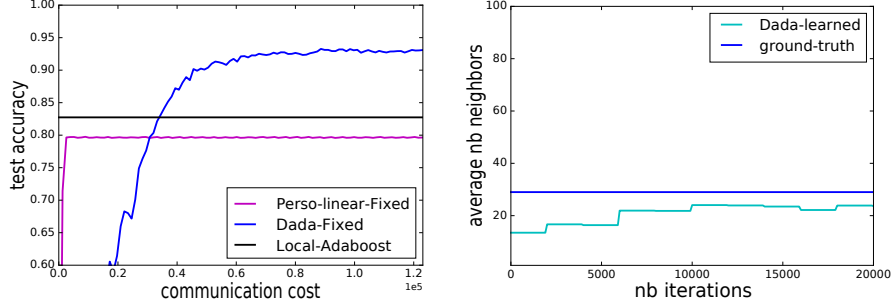


Figure 3: *Left*: Test accuracy vs communication cost in bits, *Right*: Average number of neighbors w.r.t. iterations, both on **Moons**.

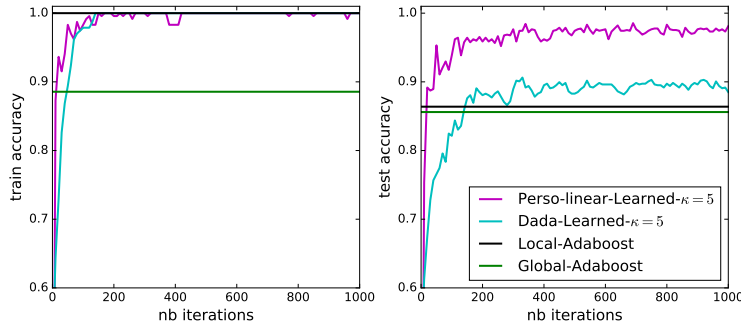


Figure 4: Training and test accuracy w.r.t. iterations on **HARWS**.

capture the specificities of the users. **Dada-Learned** and **Perso-linear-Learned**, which both make use of our alternating procedure (3), achieve the best performance. This demonstrates the wide applicability of our graph learning procedure, as it allows to use **Perso-linear** (Vanhaesebrouck et al., 2017) on datasets like **HARWS** where no prior information is available to build a fixed collaboration graph. On this rather easy problem, linear classifiers generalize better. Despite its lower accuracy at convergence, but our approach obtains better accuracy under a limited communication budget (Figure 5). The data dimension makes the communication cost of **Dada** better by 2-3 orders of magnitude: at each iteration of learning the models, $2DZ \approx 4 \times 10^4$ bits are exchanged for **Perso-linear** and only $\frac{M(Z+\log n)}{K} \approx 8 \times 10^2$ bits for **Dada**. An even larger gap holds for graph learning (10^6 versus 10^3).

More results on real datasets confirming the relevance of our approach can be found in the supplementary material.

7 Future Work

We plan to extend our approach to (functional) gradient boosting (Friedman, 2001; Wang et al., 2015) where the graph regularization term would apply to an infinite set of base predictors. Another promising direction is to make our approach differentially-private (Dwork, 2006) to formally guarantee that personal datasets cannot be inferred from the information sent by users. As our algorithm communicates very scarcely, we think that the privacy/accuracy trade-off may be better than for linear models (Bellet et al., 2018).

Acknowledgments The authors would like to thank Rémi Gilleron for his useful feedback. This research was partially supported by grants ANR-16-CE23-0016-01 and ANR-15-CE23-0026-03, and by a grant from

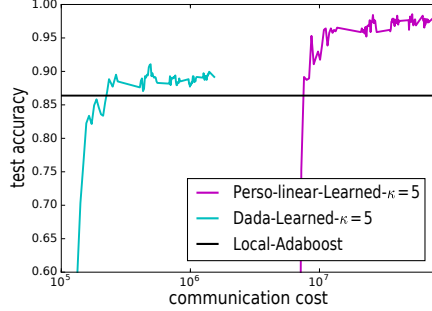


Figure 5: Test accuracy w.r.t. communication cost on **HARWS**.

CPER Nord-Pas de Calais/FEDER DATA Advanced data science and technologies 2015-2020.

References

- Anguita, D., Ghio, A., Oneto, L., Parra, X., and Reyes-Ortiz, J. L. (2013). A public domain dataset for human activity recognition using smartphones. In *ESANN*.
- Arjevani, Y. and Shamir, O. (2015). Communication complexity of distributed convex learning and optimization. In *NIPS*.
- Baytas, I. M., Yan, M., Jain, A. K., and Zhou, J. (2016). Asynchronous Multi-task Learning. In *ICDM*.
- Bekkerman, R., Bilenko, M., and Langford, J. (2011). *Scaling up machine learning: Parallel and distributed approaches*. Cambridge University Press.
- Bellet, A., Guerraoui, R., Taziki, M., and Tommasi, M. (2018). Personalized and Private Peer-to-Peer Machine Learning. In *AISTATS*.
- Bellet, A., Liang, Y., Garakani, A. B., Balcan, M.-F., and Sha, F. (2015). A distributed frank-wolfe algorithm for communication-efficient sparse learning. In *SDM*.
- Boyd, S. P., Ghosh, A., Prabhakar, B., and Shah, D. (2006). Randomized gossip algorithms. *IEEE Transactions on Information Theory*, 52(6):2508–2530.
- Clarkson, K. (2010). Coresets, sparse greedy approximation, and the frank-wolfe algorithm. *ACM Transactions on Algorithms*, 6(4):1–30.
- Colin, I., Bellet, A., Salmon, J., and Cléménçon, S. (2016). Gossip dual averaging for decentralized optimization of pairwise functions. In *ICML*.
- Cooper, J. and Reyzin, L. (2017). Improved algorithms for distributed boosting. In *Allerton*.
- Duchi, J. C., Agarwal, A., and Wainwright, M. J. (2012). Dual Averaging for Distributed Optimization: Convergence Analysis and Network Scaling. *IEEE Transactions on Automatic Control*, 57(3):592–606.
- Dwork, C. (2006). Differential Privacy. In *ICALP*, volume 2.
- Frank, M. and Wolfe, P. (1956). An algorithm for quadratic programming. *Naval Research Logistics (NRL)*, 3:95–110.
- Freund, Y. and Schapire, R. E. (1996). Experiments with a new boosting algorithm. In *ICML*.

- Freund, Y. and Schapire, R. E. (1997). A decision-theoretic generalization of on-line learning and an application to boosting. *Journal of Computer and System Sciences*, 55(1):119–139.
- Friedman, J. H. (2001). Greedy function approximation: A gradient boosting machine. *The Annals of Statistics*, 29(5):1189–1232.
- Goldstein, H. (1991). Multilevel modelling of survey data. *Journal of the Royal Statistical Society. Series D (The Statistician)*, 40(2):235–244.
- Jaggi, M. (2013). Revisiting Frank-Wolfe: Projection-Free Sparse Convex Optimization. In *ICML*.
- Jelassi, M., Voulgaris, S., Guerraoui, R., Kermarrec, A.-M., and van Steen, M. (2007). Gossip-based peer sampling. *ACM Trans. Comput. Syst.*, 25(3).
- Kalofolias, V. (2016). How to learn a graph from smooth signals. In *AISTATS*.
- Konečný, J., McMahan, H. B., Ramage, D., and Richtárik, P. (2016a). Federated Optimization: Distributed Machine Learning for On-Device Intelligence. *arXiv preprint arXiv:1610.02527*.
- Konečný, J., McMahan, H. B., Yu, F. X., Richtárik, P., Suresh, A. T., and Bacon, D. (2016b). Federated learning: Strategies for improving communication efficiency. *arXiv preprint arXiv:1610.05492*.
- Koriche, F. (2018). Compiling Combinatorial Prediction Games. In *ICML*.
- Lacoste-Julien, S., Jaggi, M., Schmidt, M., and Pletscher, P. (2013). Block-Coordinate Frank-Wolfe Optimization for Structural SVMs. In *ICML*.
- Lafond, J., Wai, H.-T., and Moulines, E. (2016). D-FW: Communication efficient distributed algorithms for high-dimensional sparse optimization. In *ICASSP*.
- Lazarevic, A. and Obradovic, Z. (2001). The distributed boosting algorithm. In *KDD*.
- Li, J., Arai, T., Baba, Y., Kashima, H., and Miwa, S. (2017). Distributed Multi-task Learning for Sensor Network. In *ECML/PKDD*.
- Lian, X., Zhang, C., Zhang, H., Hsieh, C.-J., Zhang, W., and Liu, J. (2017). Can Decentralized Algorithms Outperform Centralized Algorithms? A Case Study for Decentralized Parallel Stochastic Gradient Descent. In *NIPS*.
- Ma, C., Konečný, J., Jaggi, M., Smith, V., Jordan, M. I., Richtárik, P., and Takáč, M. (2017). Distributed optimization with arbitrary local solvers. *Optimization Methods and Software*, 32(4):813–848.
- McMahan, H. B., Moore, E., Ramage, D., Hampson, S., and Agüera y Arcas, B. (2017). Communication-efficient learning of deep networks from decentralized data. In *AISTATS*.
- Nedic, A. and Ozdaglar, A. E. (2009). Distributed Subgradient Methods for Multi-Agent Optimization. *IEEE Transactions on Automatic Control*, 54(1):48–61.
- Richtárik, P. and Takáč, M. (2014). Iteration complexity of randomized block-coordinate descent methods for minimizing a composite function. *Mathematical Programming*, 144(1-2):1–38.
- Shamir, O. and Srebro, N. (2014). Distributed Stochastic Optimization and Learning. In *Allerton*.
- Shen, C. and Li, H. (2010). On the dual formulation of boosting algorithms. *IEEE Transactions on Pattern Analysis and Machine Intelligence*, 32(12):2216–2231.
- Smith, V., Chiang, C.-K., Sanjabi, M., and Talwalkar, A. S. (2017). Federated Multi-Task Learning. In *NIPS*.

- Song, Y., Lu, Z., Leung, C. W.-k., and Yang, Q. (2013). Collaborative boosting for activity classification in microblogs. In *KDD*.
- Suresh, A. T., Yu, F. X., Kumar, S., and McMahan, H. B. (2017). Distributed Mean Estimation with Limited Communication. In *ICML*.
- Tang, H., Gan, S., Zhang, C., Zhang, T., and Liu, J. (2018a). Communication Compression for Decentralized Training. In *NeurIPS*.
- Tang, H., Lian, X., Yan, M., Zhang, C., and Liu, J. (2018b). D^2 : Decentralized Training over Decentralized Data. In *ICML*.
- Vanhaesebrouck, P., Bellet, A., and Tommasi, M. (2017). Decentralized Collaborative Learning of Personalized Models over Networks. In *AISTATS*.
- Wang, C., Wang, Y., Schapire, R., et al. (2015). Functional Frank-Wolfe Boosting for General Loss Functions. *arXiv preprint arXiv:1510.02558*.
- Wang, J., Kolar, M., and Srebro, N. (2016a). Distributed Multi-Task Learning with Shared Representation. *arXiv preprint arXiv:1603.02185*.
- Wang, J., Kolar, M., and Srebro, N. (2016b). Distributed Multitask Learning. In *AISTATS*.
- Wang, S. and Zhang, C. (2005). Network game and boosting. In *ECML*.
- Wei, E. and Ozdaglar, A. E. (2012). Distributed Alternating Direction Method of Multipliers. In *CDC*.
- Wright, S. J. (2015). Coordinate descent algorithms. *Mathematical Programming*, 151(1):3–34.
- Zhang, Y., Duchi, J. C., Jordan, M. I., and Wainwright, M. J. (2013). Information-theoretic lower bounds for distributed statistical estimation with communication constraints. In *NIPS*.
- Zhang, Y., Wainwright, M. J., and Duchi, J. C. (2012). Communication-efficient algorithms for statistical optimization. In *NIPS*.

SUPPLEMENTARY MATERIAL

This supplementary material is organized as follows. Section Appendix A provides the convergence analysis for our decentralized Frank-Wolfe boosting algorithm. Section Appendix B describes the convergence analysis of our decentralized graph learning algorithm. Section Appendix C derives the expected communication cost of the algorithm when agents can keep in memory the models of all the agents they communicate with. Finally, Section Appendix D presents additional experimental results.

Appendix A Proof of Theorem 1

We first recall our joint optimization problem over the classifiers $\alpha = [\alpha_1, \dots, \alpha_K] \in (\mathbb{R}^n)^K$:

$$\min_{\|\alpha_1\|_1 \leq \beta, \dots, \|\alpha_K\|_1 \leq \beta} f(\alpha) = \sum_{k=1}^K d_k c_k \log \left(\frac{1}{m_k} \sum_{i=1}^{m_k} \exp(-(\mathbf{A}_k \alpha_k)_i) \right) + \frac{\mu}{2} \sum_{k=1}^K \sum_{l=1}^{k-1} w_{k,l} \|\alpha_k - \alpha_l\|^2. \quad (7)$$

We recall some notations. For any $k \in [K]$, we let $\mathcal{M}^k = \{\alpha_k \in \mathbb{R}^n : \|\alpha_k\|_1 \leq \beta\}$ and denote by $\mathcal{M} = \mathcal{M}^1 \times \dots \times \mathcal{M}^K$ our feasible domain in (7). We also denote by $v_{[k]} \in \mathcal{M}$ the zero-padding of any vector $v_k \in \mathcal{M}^k$. Finally, for conciseness of notations, for a given $\gamma \in [0, 1]$ we write $\hat{\alpha} = \alpha + \gamma(s_{[k]} - \alpha_{[k]})$ and $\hat{\alpha}_k = (1 - \gamma)\alpha_k + \gamma s_k$.

A.1 Curvature Bound

We first show that our objective function satisfies a form of smoothness over the feasible domain, which is expressed by a notion of curvature. Precisely, the global product curvature constant C_f^\otimes of f over \mathcal{M} is the sum over each block of the maximum relative deviation of f from its linear approximations over the block Lacoste-Julien et al. (2013):

$$C_f^\otimes = \sum_{k=1}^K C_f^k = \sum_{k=1}^K \sup_{\substack{\alpha \in \mathcal{M}, s_k \in \mathcal{M}^k \\ \gamma \in [0, 1]}} \left\{ \frac{2}{\gamma^2} (f(\hat{\alpha}) - f(\alpha) - (\hat{\alpha}_k - \alpha_k)^\top \nabla_k f(\alpha)) \right\}. \quad (8)$$

We will use the fact that each partial curvature constant C_f^k is upper bounded by the (block) Lipschitz constant of the partial gradient $\nabla_k f(\alpha)$ times the squared diameter of the blockwise feasible domain \mathcal{M}^k Lacoste-Julien et al. (2013). The next lemma gives a bound on the product space curvature C_f^\otimes .

Lemma 1. *For Problem (7), we have $C_f^\otimes \leq 4\beta^2 \sum_{k=1}^K (d_k c_k \|\mathbf{A}_k\|_1^2 + \mu d_k)$.*

Proof. For the following proof, we rely on two key concepts: the Lipschitz continuity and the diameter of a compact space. A function $f : \mathcal{X} \rightarrow \mathbb{R}$ is L -lipschitz w.r.t. the norm $\|\cdot\|_1$ if $\forall (x, x') \in \mathcal{X}^2$:

$$|f(x) - f(x')| \leq L \|x - x'\|_1. \quad (9)$$

The diameter of a compact normed vector space $(\mathcal{M}, \|\cdot\|)$ is defined as:

$$\text{diam}_{\|\cdot\|}(\mathcal{M}) = \sup_{x, x' \in \mathcal{M}} \|x - x'\|. \quad (10)$$

We recall the expression for the partial gradient:

$$\nabla_k f(\alpha) = -d_k c_k \eta_k(\alpha)^\top \mathbf{A}_k + \mu \left(d_k \alpha_{[k]} - \sum_l w_{k,l} \alpha_{[l]} \right),$$

where we denote $\eta_k(\alpha) = \frac{\exp(-\mathbf{A}_k \alpha_{[k]})}{\sum_{i=1}^{m_k} \exp(-\mathbf{A}_k \alpha_{[k]})_i}$.

We bound the Lipschitz constant of $\eta_k(\alpha)$ by bounding its first derivative:

$$\begin{aligned}\|\nabla_k(\eta_k(\alpha))\|_1 &= \|(-\eta_k(\alpha) + \eta_k(\alpha)^2)^\top A_k\|_1 \\ &\leq \|A_k\|_1.\end{aligned}\tag{11}$$

Eq. (11) is due to the fact that $\|\eta_k(\alpha)\|_1 \leq 1$ and $\eta_k(\alpha) \geq 0$. It is then easy to see that considering any two vectors $\alpha, \alpha' \in \mathcal{M}$ differing only in their k -th block ($\alpha_{[l]} = \alpha'_{[l]} \forall l \neq k$), the Lipschitz constant of the partial gradient $\nabla_k f$ in (11) is bounded by $L_k = d_k c_k \|A_k\|_1^2 + \mu d_k$.

We can easily bound the diameter of the subspace $\mathcal{M}^k = \{\alpha_k \in \mathbb{R}^n : \|\alpha_k\|_1 \leq \beta\}$ as follows:

$$\text{diam}_{\|\cdot\|_1}(\mathcal{M}^k) = \max_{\alpha_k, \alpha'_k \in \mathcal{M}^k} \|\alpha_k - \alpha'_k\|_1 = 2\beta.$$

Finally, we obtain Lemma 1 by combining the above results:

$$C_f^\otimes = \sum_{k=1}^K C_f^k \leq \sum_{k=1}^K L_k \text{diam}_{\|\cdot\|_1}^2(\mathcal{M}^k) = 4\beta^2 \sum_{k=1}^K (d_k c_k \|A_k\|_1^2 + \mu d_k).\tag{12}$$

□

A.2 Convergence Analysis

We can now prove the convergence rate of our algorithm by following the proof technique proposed by Jaggi in Jaggi (2013) and refined by Lacoste-Julien et al. (2013) for the case of block coordinate Frank-Wolfe.

We start by introducing some useful notation related to our problem (7):

$$\begin{aligned}\text{gap}(\alpha) &= \max_{s \in \mathcal{M}} \{(\alpha - s)^\top \nabla(f(\alpha))\} = \sum_{k=1}^K \text{gap}_k(\alpha_k) \\ &= \sum_{k=1}^K \max_{s_k \in \mathcal{M}^k} \{(\alpha_k - s_k)^\top \nabla_k f(\alpha)\}\end{aligned}\tag{13}$$

The quantity $\text{gap}(\alpha)$ can serve as a certificate for the quality of a current approximation of the optimum of the objective function (Jaggi, 2013). In particular, one can show that $f(\alpha) - f(\alpha^*) \leq \text{gap}(\alpha)$ where α^* is a solution of (7). Under a bounded global product curvature constant C_f^\otimes , we will obtain the convergence of Frank-Wolfe by showing that the surrogate gap decreases in expectation over the iterations, because at a given iteration t the block-wise surrogate gap at the current solution $\text{gap}_k(\alpha_k^{(t)})$ is minimized by the greedy update $s_k^{(t)} \in \mathcal{M}^k$.

Using the definition of the curvature (8) and rewriting $\hat{\alpha}_k - \alpha_k = -\gamma_k(\alpha_k - s_k)$, we obtain

$$f(\hat{\alpha}) \leq f(\alpha) - \gamma(\alpha_k - s_k)^\top \nabla_k f(\alpha) + \gamma^2 \frac{C_f^k}{2}.$$

In particular, at any iteration t , the previous inequality holds for $\gamma = \gamma^{(t)} = \frac{2K}{t+2K}$, $\alpha^{(t+1)} = \alpha^{(t)} + \gamma^{(t)}(s_k^{(t+1)} - \alpha_k^{(t+1)})$ with $s_k^{(t+1)} = \arg \min_{s \in \mathcal{M}^k} \{s^\top \nabla_k f(\alpha^{(t)})\}$ as defined in (2). Therefore, $(\alpha_k - s_k)^\top \nabla_k f(\alpha)$ is by definition $\text{gap}_k(\alpha_k)$ and

$$f(\alpha^{(t+1)}) \leq f(\alpha^{(t)}) - \gamma^{(t)} \text{gap}_k(\alpha_k^{(t)}) + (\gamma^{(t)})^2 \frac{C_f^k}{2}.$$

By taking the expectation over the random choice of $k \sim \mathcal{U}(1, K)$ on both sides, we obtain

$$\begin{aligned}\mathbb{E}_k[f(\alpha^{(t+1)})] &\leq \mathbb{E}_k[f(\alpha^{(t)})] - \gamma^{(t)} \mathbb{E}_k[\text{gap}_k(\alpha_k^{(t)})] + \frac{(\gamma^{(t)})^2 \mathbb{E}_k[C_f^k]}{2} \\ &\leq \mathbb{E}_k[f(\alpha^{(t)})] - \frac{\gamma^{(t)} \text{gap}(\alpha^{(t)})}{K} + \frac{(\gamma^{(t)})^2 C_f^\otimes}{2K}.\end{aligned}\tag{14}$$

Let us define the sub-optimality gap $p(\alpha) = f(\alpha) - f^*$ with f^* the optimal value of f . By subtracting f^* from both sides in (14), we obtain

$$\mathbb{E}_k[p(\alpha^{(t+1)})] \leq \mathbb{E}_k[p(\alpha^{(t)})] - \frac{\gamma^{(t)}}{K} \mathbb{E}_k[p(\alpha^{(t)})] + (\gamma^{(t)})^2 \frac{C_f^\otimes}{2K} \quad (15)$$

$$\leq \left(1 - \frac{\gamma^{(t)}}{K}\right) \mathbb{E}_k[p(\alpha^{(t)})] + (\gamma^{(t)})^2 \frac{C_f^\otimes}{2K}. \quad (16)$$

Inequality (15) comes from the definition of the surrogate gap (13) which ensures that $\mathbb{E}_k[p(\alpha)] \leq \text{gap}(\alpha)$.

Therefore, we can show by induction that the expected sub-optimality gap satisfies $\mathbb{E}_k[p(\alpha^{(t+1)})] \leq \frac{2K(C_f^\otimes + p_0)}{t+2K}$, with $p_0 = p(\alpha^{(0)})$ the initial gap. This shows that the expected sub-optimality gap $\mathbb{E}_k[p(\alpha)]$ decreases with the number of iterations with a rate $O(\frac{1}{t})$, which implies the convergence of our algorithm to the optimal solution. The final convergence rate can then be obtained by the same proof as Lacoste-Julien et al. (2013) (Appendix C.3 therein) combined with Lemma 1.

Appendix B Proof of Theorem 2

We start by computing the (block) smoothness and strong convexity parameters of the objective function $h(w)$ (Section B.1). We then show that our algorithm can be explicitly formulated as an instance of proximal block coordinate descent (Section B.2). Building upon this formulation, we prove the convergence rate in Section B.3.

B.1 Smoothness and Strong Convexity

Smoothness. A function $f : \mathcal{X} \rightarrow \mathbb{R}$ is L -smooth w.r.t. the Euclidean norm if its gradient is L -Lipschitz, i.e. $\forall (x, x') \in \mathcal{X}^2$:

$$\|\nabla f(x) - \nabla f(x')\| \leq L\|x - x'\|.$$

In our case, we need to analyze the smoothness of our objective function h for each block of coordinates indexed by (k, \mathcal{K}) , i.e. for any $(w, w') \in \mathbb{R}_+^{K(K-1)/2}$ which differ only in the (k, \mathcal{K}) -block, we want to find $L_{k, \mathcal{K}}$ such that:

$$\|[\nabla h(w)]_{k, \mathcal{K}} - [\nabla h(w')]_{k, \mathcal{K}}\| \leq L_{k, \mathcal{K}} \|w_{k, \mathcal{K}} - w'_{k, \mathcal{K}}\|.$$

Lemma 2. For any block (k, \mathcal{K}) of size κ , we have $L_\kappa := L_{k, \mathcal{K}} \leq 2\mu(\frac{\kappa+1}{\delta^2} + \lambda)$

Proof. Recall from the main text that the partial gradient can be written as follows:

$$[\nabla h(w)]_{k, \mathcal{K}} = p_{k, \mathcal{K}} + \mu \left(\frac{1}{2} \Delta_{k, \mathcal{K}} - v_{k, \mathcal{K}} + 2\lambda w_{k, \mathcal{K}} \right). \quad (17)$$

The first two terms do not depend on $w_{k, \mathcal{K}}$ and can thus be ignored. We focus on the Lipschitz constant corresponding to the third term. Let $(w, w') \in \mathbb{R}_+^{K(K-1)/2}$ such that they only differ in the block indexed by (k, \mathcal{K}) . We denote the degree of an agent k with respect to w and w' by $d_k = \sum_j w_{k,j}$ and $d'_k = \sum_j w'_{k,j}$ respectively. We have:

$$\begin{aligned}
\|v_{k,\mathcal{K}} - v'_{k,\mathcal{K}}\| &= \left\| \left(\frac{1}{d_k + \delta} + \frac{1}{d_l + \delta} \right)_{l \in \mathcal{K}} - \left(\frac{1}{d'_k + \delta} + \frac{1}{d'_l + \delta} \right)_{l \in \mathcal{K}} \right\| \\
&= \left\| \left(\frac{d'_k + \delta - d_k - \delta}{(d_k + \delta)(d'_k + \delta)} + \frac{d'_l + \delta - d_l - \delta}{(d_l + \delta)(d'_l + \delta)} \right)_{l \in \mathcal{K}} \right\| \\
&\leq \frac{1}{\delta^2} \left\| \left(\sum_{j \in \mathcal{K}} (w'_{k,j} - w_{k,j}) \right)_{l \in \mathcal{K}} + (w'_{k,l} - w_{k,l})_{l \in \mathcal{K}} \right\| \tag{18}
\end{aligned}$$

$$\begin{aligned}
&\leq \frac{1}{\delta^2} \left[\left\| \left(\|w'_{k,\mathcal{K}}\|_1 - \|w_{k,\mathcal{K}}\|_1 \right)_{l \in \mathcal{K}} \right\| + \|w_{k,\mathcal{K}} - w'_{k,\mathcal{K}}\| \right] \\
&\leq \frac{1}{\delta^2} \left[\left\| \left(\|w'_{k,\mathcal{K}} - w_{k,\mathcal{K}}\|_1 \right)_{l \in \mathcal{K}} \right\| + \|w_{k,\mathcal{K}} - w'_{k,\mathcal{K}}\| \right] \tag{19}
\end{aligned}$$

$$\leq \frac{1}{\delta^2} \left[\sqrt{\kappa} \left| \sum_{j \in \mathcal{K}} (w'_{k,j} - w_{k,j}) \right| + \|w_{k,\mathcal{K}} - w'_{k,\mathcal{K}}\| \right] \tag{20}$$

$$\leq \frac{1}{\delta^2} \left[\sqrt{\kappa} \|w_{k,\mathcal{K}} - w'_{k,\mathcal{K}}\|_1 + \|w_{k,\mathcal{K}} - w'_{k,\mathcal{K}}\| \right] \tag{21}$$

$$\leq \frac{\kappa + 1}{\delta^2} \|w_{k,\mathcal{K}} - w'_{k,\mathcal{K}}\|,$$

where to obtain (18) we used the nonnegativity of the weights and the fact that w and w' only differ in the coordinates indexed by (k, \mathcal{K}) , and (19)-(20)-(21) by classic properties of norms.

We conclude by combining this result with the quantity 2λ that comes from the last term in (17) and multiplying by μ . Since $L_{k,\mathcal{K}}$ only depends on the block size κ (not the block itself), we will simply denote $L_\kappa := L_{k,\mathcal{K}}$. \square

It is important to note that the linear dependency of L_κ in the block size κ , which is the worst possible dependency for block Lipschitz constants (Wright, 2015), is in fact *tight* for our objective function. This is due to the log-degree term which makes each entry of $[\nabla h(w)]_{k,\mathcal{K}}$ dependent on the sum of all coordinates in $w_{k,\mathcal{K}}$. This linear dependency explains the mild effect of the block size κ on the convergence rate of our algorithm (see Theorem 2 and the discussion of Section 4.4).

Strong convexity. It is easy to see that the objective function h is σ -strongly convex with $\sigma = 2\mu\lambda$.

B.2 Interpretation as Proximal Coordinate Descent

First, we reformulate our graph learning subproblem as an equivalent unconstrained optimization problem by incorporating the nonnegativity constraints into the objective:

$$\min_{w \in \mathbb{R}^{K(K-1)/2}} F(w) = h(w) + r(w), \tag{22}$$

where

$$h(w) = \sum_{k=1}^K d_k c_k \mathcal{L}_k(\alpha_k; S_k) + \mu \left(\frac{1}{2} \sum_{k < l} w_{k,l} \|\alpha_k - \alpha_l\|^2 - \mathbf{1}^\top \log(d + \delta) + \lambda \|w\|^2 \right), \tag{23}$$

$$r(w) = \sum_{k < l} \mathbb{I}_{\geq 0}(w_{k,l}). \tag{24}$$

In the expression above, $\mathbb{I}_{\geq 0}$ denotes the characteristic function of the nonnegative orthant of \mathbb{R} : $\mathbb{I}_{\geq 0}(x) = 0$ if $x \geq 0$ and $+\infty$ otherwise. We know that $h(w)$ is strongly convex and smooth (see Section B.1 for the derivation of smoothness and strong convexity parameters), while it is clear that $r(w)$ is not smooth but convex and separable across the coordinates of w . We will denote by w^* the solution to (22), which is also the solution to our original (constrained) graph learning subproblem.

We will now show that the algorithm presented in the main text can be explicitly reformulated as an instance of proximal block coordinate descent (Richtárik and Takáć, 2014) applied to the function $F(w)$. In the process, we will introduce some notations that we will reuse in the convergence analysis provided in Section B.3. At each iteration t , a random block of coordinates indexed by (k, \mathcal{K}) is selected. Consider the following update:

$$\begin{cases} z_{k, \mathcal{K}}^{(t)} \leftarrow \arg \min_{z \in \mathbb{R}^\kappa} \left\{ (z - w_{k, \mathcal{K}}^{(t)})^\top [\nabla h(w^{(t)})]_{k, \mathcal{K}} + \frac{L_\kappa}{2} \|z - w_{k, \mathcal{K}}^{(t)}\|^2 + \sum_{l \in \mathcal{K}} \mathbb{I}_{\geq 0}(z_{k, l}) \right\} \\ w^{(t+1)} \leftarrow w^{(t)} + U_{k, \mathcal{K}}(z_{k, \mathcal{K}}^{(t)} - w_{k, \mathcal{K}}^{(t)}) \end{cases} \quad (25)$$

For notational convenience, $U_{k, \mathcal{K}}$ denotes the column submatrix of the $K(K-1)/2 \times K(K-1)/2$ identity matrix such that $w^\top U_{k, \mathcal{K}} = w_{k, \mathcal{K}} \in \mathbb{R}^{\kappa}$ for any $w \in \mathbb{R}^{K(K-1)/2}$.

Notice that the minimization problem in (25) is separable and can be solved independently for each coordinate. Denoting by

$$\tilde{z}^{(t)} = \arg \min_{z \in \mathbb{R}^{K(K-1)/2}} \left\{ (z - w^{(t)})^\top \nabla h(w^{(t)}) + \frac{L_\kappa}{2} \|z - w^{(t)}\|^2 + r(z) \right\}, \quad (26)$$

we can thus rewrite (25) as:

$$w_{j, l}^{(t+1)} = \begin{cases} \tilde{z}_{j, l}^{(t)} & \text{if } j = k \text{ and } l \in \mathcal{K} \\ w_{j, l}^{(t)} & \text{otherwise} \end{cases} \quad (27)$$

Finally, recalling the definition of the proximal operator of a function f :

$$\text{prox}_f(w) = \arg \min_z \left\{ f(z) + \frac{1}{2} \|w - z\|^2 \right\},$$

we can rewrite (26) as:

$$\tilde{z}^{(t)} = \text{prox}_{\frac{1}{L_\kappa} r}(w^{(t)} - (1/L_\kappa) \nabla h(w^{(t)})). \quad (28)$$

We have indeed obtained that (27) corresponds to a proximal block coordinate descent update (Richtárik and Takáć, 2014), i.e. a proximal gradient descent step restricted to a block of coordinates.

When f is the characteristic function of a set, the proximal operator corresponds to the Euclidean projection onto the set. Hence, in our case we have $\text{prox}_r(w) = \max(0, w)$ (the thresholding operator), and we recover the simple update (5) introduced in the main text.

B.3 Convergence Analysis

We start by introducing a convenient lemma.

Lemma 3. *For any block of size κ indexed by (k, \mathcal{K}) , any $w \in \mathbb{R}^{K(K-1)/2}$ and any $z \in \mathbb{R}^\kappa$, we have:*

$$h(w + U_{k, \mathcal{K}} z) \leq h(w) + z^\top [\nabla h(w)]_{k, \mathcal{K}} + \frac{L_\kappa}{2} \|z\|^2.$$

Proof. This is obtained by applying Taylor's inequality to the function

$$\begin{aligned} q_w : \mathbb{R}^\kappa &\rightarrow \mathbb{R} \\ z &\mapsto h(w + U_{k, \mathcal{K}} z) \end{aligned}$$

combined with the convexity and L_κ -block smoothness of h . \square

We are now ready to prove the convergence rate of our algorithm. We focus below on the more interesting cases where the block size $\kappa > 1$, since the case $\kappa = 1$ (blocks of size 1) reduces to standard proximal coordinate descent and can be addressed directly by previous work (Richtárik and Takáć, 2014; Wright, 2015).

Recall that in our algorithm, at each iteration an agent k is drawn uniformly at random from $[K]$, and then this agent samples a set \mathcal{K} of κ other agents uniformly and without replacement from the set $\{1, \dots, K\} \setminus \{k\}$. This gives rise to a block of coordinates indexed by (k, \mathcal{K}) . Let \mathcal{B} be the set of such possible block indices. Note that \mathcal{B} has cardinality $K \binom{K-1}{\kappa}$ since for $\kappa > 1$ all $\binom{K-1}{\kappa}$ blocks that can be sampled by an agent are unique (i.e., they cannot be sampled by other agents). However, it is important to note that unlike commonly assumed in the block coordinate descent literature, our blocks exhibit an overlapping structure: each coordinate block $b \in \mathcal{B}$ shares some of its coordinates with several other blocks in \mathcal{B} . In particular, each coordinate (graph weight) $w_{i,j}$ is shared by agent i and agent j can thus be part of blocks drawn by both agents. Our analysis builds upon the proof technique of Wright (2015), adapting the arguments to handle our update structure based on overlapping blocks rather than single coordinates.

Let $b_t = (k, \mathcal{K}) \in \mathcal{B}$ be the block of coordinates selected at iteration t . For notational convenience, we write $(j, l) \in b_t$ to denote the set of coordinates indexed by block b_t (i.e., index pairs (j, l) such that $j = k$ and $l \in \mathcal{K}$). Consider the expectation of the objective function $F(w^{(t+1)})$ in (22) over the choice of b_t , plugging in the update (25):

$$\begin{aligned} \mathbb{E}_{b_t}[F(w^{(t+1)})] &= \mathbb{E}_{b_t} \left[h(w^{(t)} + U_{b_t}(z_{b_t}^{(t)} - w_{b_t}^{(t)})) + \sum_{(j,l) \in b_t} \mathbb{I}_{\geq 0}(z_{j,l}^{(t)}) + \sum_{(j,l) \notin b_t} \mathbb{I}_{\geq 0}(w_{j,l}^{(t)}) \right] \\ &= \frac{1}{K \binom{K-1}{\kappa}} \sum_{b \in \mathcal{B}} \left[h(w^{(t)} + U_b(z_b^{(t)} - w_b^{(t)})) + \sum_{(j,l) \in b} \mathbb{I}_{\geq 0}(z_{j,l}^{(t)}) + \sum_{(j,l) \notin b} \mathbb{I}_{\geq 0}(w_{j,l}^{(t)}) \right] \\ &\leq \frac{1}{K \binom{K-1}{\kappa}} \sum_{b \in \mathcal{B}} \left[h(w^{(t)}) + (z_b^{(t)} - w_b^{(t)})^\top [\nabla h(w^{(t)})]_b + \frac{L_\kappa}{2} \|z_b^{(t)} - w_b^{(t)}\|^2 \right. \\ &\quad \left. + \sum_{(j,l) \in b} \mathbb{I}_{\geq 0}(z_{j,l}^{(t)}) + \sum_{(j,l) \notin b} \mathbb{I}_{\geq 0}(w_{j,l}^{(t)}) \right], \end{aligned} \tag{29}$$

where we have used Lemma 3 to obtain (29), and $z_b^{(t)}$ is defined as in (25) for any block $b = (k, \mathcal{K})$.

We now need to aggregate the blocks over the sum in (29), taking into account the overlapping structure of our blocks. We rely on the observation that each coordinate $w_{k,l}$ appears in exactly $2 \binom{K-2}{\kappa-1}$ blocks. Grouping coordinates accordingly in (29) gives:

$$\begin{aligned} \mathbb{E}_{b_t}[F(w^{(t+1)})] &\leq \frac{K \binom{K-1}{\kappa} - \kappa \binom{K-2}{\kappa-1}}{K \binom{K-1}{\kappa}} F(w^{(t)}) \\ &\quad + \frac{\kappa \binom{K-2}{\kappa-1}}{K \binom{K-1}{\kappa}} \left(h(w^{(t)}) + (\tilde{z}^{(t)} - w^{(t)})^\top \nabla h(w^{(t)}) + \frac{L_\kappa}{2} \|\tilde{z}^{(t)} - w^{(t)}\|^2 + r(\tilde{z}^{(t)}) \right), \end{aligned} \tag{30}$$

where $\tilde{z}^{(t)}$ is defined as in (26). This is because the block b of $\tilde{z}^{(t)}$ is equal to $z_b^{(t)}$, as explained in Section B.2.

We now deal with the second term in (30). Let us consider the following function H :

$$H(w^{(t)}, z) = h(w^{(t)}) + (z - w^{(t)})^\top \nabla h(w^{(t)}) + \frac{L_\kappa}{2} \|z - w^{(t)}\|^2 + r(z).$$

By σ -strong convexity of h , we have:

$$\begin{aligned} H(w^{(t)}, z) &\leq h(z) - \frac{\sigma}{2} \|z - w^{(t)}\|^2 + \frac{L_\kappa}{2} \|z - w^{(t)}\|^2 + r(z) \\ &= F(z) + \frac{1}{2} (L_\kappa - \sigma) \|z - w^{(t)}\|^2. \end{aligned} \tag{31}$$

Note that H achieves its minimum at $\tilde{z}^{(t)}$ defined in (26). If we minimize over z both sides of (31) we get

$$\begin{aligned} H(w^{(t)}, \tilde{z}^{(t)}) &= \min_z H(w^{(t)}, z) \\ &\leq \min_z F(z) + \frac{1}{2} (L_\kappa - \sigma) \|z - w^{(t)}\|^2. \end{aligned}$$

By σ -strong convexity of F ,³ we have for any w, w' and $\alpha \in [0, 1]$:

$$F(\alpha w + (1 - \alpha)w') \leq \alpha F(w) + (1 - \alpha)F(w') - \frac{\sigma\alpha(1 - \alpha)}{2}\|w - w'\|^2. \quad (32)$$

Using the change of variable $z = \alpha w^* + (1 - \alpha)w^{(t)}$ for $\alpha \in [0, 1]$ and (32) we obtain:

$$\begin{aligned} H(w^{(t)}, \tilde{z}^{(t)}) &\leq \min_{\alpha \in [0, 1]} F(\alpha w^* + (1 - \alpha)w^{(t)}) + \frac{1}{2}(L_\kappa - \sigma)\alpha^2\|w^* - w^{(t)}\|^2 \\ &\leq \min_{\alpha \in [0, 1]} \alpha F(w^*) + (1 - \alpha)F(w^{(t)}) + \frac{1}{2}[(L_\kappa - \sigma)\alpha^2 - \sigma\alpha(1 - \alpha)]\|w^* - w^{(t)}\|^2 \end{aligned} \quad (33)$$

$$\leq \frac{\sigma}{L_\kappa}F(w^*) + \left(1 - \frac{\sigma}{L_\kappa}\right)F(w^{(t)}), \quad (34)$$

where the last inequality is obtained by plugging the value $\alpha = \sigma/L_\kappa$, which cancels the last term in (33).

We can now plug (34) into (30) and subtract $F(w^*)$ on both sides to get:

$$\begin{aligned} \mathbb{E}_{b_t}[F(w^{(t+1)})] - F(w^*) &\leq \frac{K\binom{K-1}{\kappa} - 2\binom{K-2}{\kappa-1}}{K\binom{K-1}{\kappa}}F(w^{(t)}) + \frac{2\binom{K-2}{\kappa-1}}{K\binom{K-1}{\kappa}}\left(\frac{\sigma}{L_\kappa}F(w^*) + \left(1 - \frac{\sigma}{L_\kappa}\right)F(w^{(t)})\right) \\ &= \left(1 - \frac{2\kappa\sigma}{K(K-1)L_\kappa}\right)(F(w^{(t)}) - F(w^*)), \end{aligned} \quad (35)$$

where we used the fact that $\frac{2\binom{K-2}{\kappa-1}}{K\binom{K-1}{\kappa}} = \frac{2\kappa}{K(K-1)}$. We conclude by taking the expectation of both sides with respect to the choice of previous blocks b_0, \dots, b_{t-1} followed by a recursive application of the resulting formula, and finally plugging in the strong convexity and smoothness parameters obtained in Section B.1.

Appendix C Expected Communication Cost for Graph Learning

As noted in Section 4.4, the communication complexity of our decentralized graph learning algorithm can be reduced if the agents store the models and local losses of all the peers they communicate with. The communication complexity for a given iteration t then depends on the expected number of nodes $\kappa^{(t)}$, among the selected \mathcal{K} , that the picked agent has not yet selected:

$$\kappa 2Z + \kappa^{(t)} \left(Z + \min\left(\frac{t_\alpha}{K}, n\right)(Z + \log n) \right).$$

The next lemma shows that $\kappa^{(t)}$ decreases exponentially fast with the number of iterations.

Lemma 4. *For any $T \geq 1$, the expected number of new nodes after T iterations is given by*

$$\kappa^{(T)} = \kappa \left(1 - \frac{\kappa}{K(K-1)}\right)^{T-1}.$$

Proof. At a given iteration t , let $k^{(t)}$ denote the random agent that performs the update and $\mathcal{K}^{(t)}$ the set of κ agents selected by $k^{(t)}$. We denote by $X_{l,m}^{(t)}$ the random variable indicating if node l selected node m at that iteration:

$$X_{l,m}^{(t)} = \begin{cases} 0 & \text{if node } m \text{ was not selected by node } l \text{ at iteration } t, \\ 1 & \text{otherwise.} \end{cases}$$

Similarly, $X_{l,m}$ indicates if node l has ever selected node m after T iterations.

³ $F = h + r$ is σ -strongly convex since h is σ -strongly convex and r is convex.

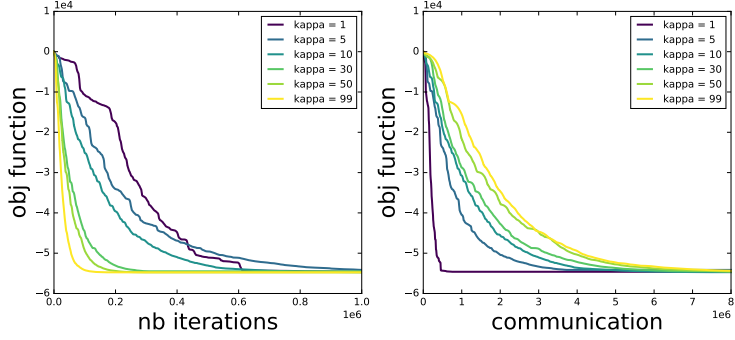


Figure 6: Impact of κ on the convergence rate and the communication cost for learning the graph on **Moons**.

Let us denote by $R^{(t)} = \{X_{k^{(t)},j}\}_{j \in \mathcal{K}^{(t)}}$ the set of random variables that have to be updated at iteration t . The probability that node m is not selected by node l at a given round t is given by

$$\begin{aligned} \mathbb{P}[X_{l,m}^{(t)} = 0] &= \mathbb{P}[k^{(t)} = l] \mathbb{P}[X_{k^{(t)},m} \notin R^{(t)} | k^{(t)} = l] + \mathbb{P}[k^{(t)} \neq l] \mathbb{P}[X_{k^{(t)},m} \notin R^{(t)} | k^{(t)} \neq l] \\ &= \frac{1}{K} \left(1 - \frac{\kappa}{K-1}\right) + \frac{K-1}{K} 1 \\ &= \frac{K^2 - K - \kappa}{K(K-1)} = 1 - \frac{\kappa}{K(K-1)}. \end{aligned}$$

As k and \mathcal{K} are drawn independently from the previous draws, the probability that node m has never been selected by node l after T iterations is given by:

$$\mathbb{P}[X_{l,m} = 0] = \prod_{t=0}^{T-1} \mathbb{P}[X_{l,m}^{(t)} = 0] = \left(1 - \frac{\kappa}{K(K-1)}\right)^T.$$

Finally, the expected number of new nodes seen at iteration T is given by

$$\kappa^{(T)} = \mathbb{E}_{k,\mathcal{K}}[\ |\{X_{k,l} \in R^{(T)} | X_{k,l} = 0\}|\] = \frac{1}{K} \sum_{k=1}^K \frac{1}{\binom{K-1}{\kappa}} \sum_{\mathcal{K}} \sum_{m \in \mathcal{K}} \mathbb{P}[X_{l,m} = 0] = \kappa \left(1 - \frac{\kappa}{K(K-1)}\right)^{T-1}.$$

□

Appendix D Additional Experimental Results

D.1 Effect of the Block Size κ

As discussed in Section 4.4, the parameter κ allows to trade-off the communication cost (in bits as well as the number of pairwise connections at each iteration) and the convergence rate for the graph learning steps of **Dada-Learned**. We study the effect of varying κ on **Moons**, the synthetic dataset used in Section 6.1. Figure 6 shows the evolution of the objective function with the number of iterations and with the communication cost depending on κ when learning a graph using the local classifiers learned with **Local-Adaboost**. Notice that the numerical behavior is consistent with the theory: while increasing κ reduces the number of communication rounds, setting $\kappa = 1$ minimizes the total amount of communication (about 5×10^5 bits). By way of comparison, the communication cost required to send all weights to all agents just once is $ZK^2(K-1)/2 = 1.6 \times 10^7$ bits. In practice, moderate values of κ can be used to obtain a good trade-off between the number of rounds and the total communication cost, and to reduce the higher variance associated with small values of κ .

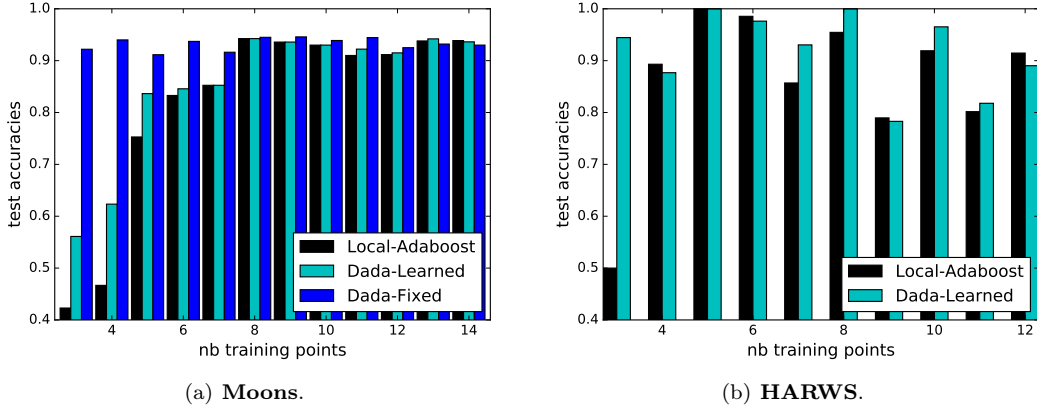


Figure 7: Average test accuracies with respect to the number of training points of the local sets.

D.2 Test Accuracy w.r.t. Local Dataset Size

In the main text, the reported accuracies were averaged over agents. Here, we study the relation between the local test accuracy of agents in **Dada** depending on the size of their training set. Figure 7 shows a comparison between **Dada** and **Local-Adaboost**, in order to assess the improvements introduced by our collaborative scheme. On **Moons**, **Local-Adaboost** shows good performance on agents with larger training sets but generalizes poorly on agents with limited local information. Both **Dada-Fixed** and **Dada-Learned** outperform **Local-Adaboost**, especially on agents with small datasets. Remarkably, in the ideal setting where we have access to the ground-truth graph (**Dada-Fixed**), we are able to fully close the accuracy gaps caused by uneven training set sizes. **Dada-Learned** is able to match this performance except on agents with smaller datasets, which is expected since there is very limited information available to learn reliable similarity weights for these agents. On **HARWS**, **Dada-Learned** generally improves upon **Local-Adaboost**, although there is more variability due to difference in difficulty across user tasks and uneven numbers of agents in each size group.

D.3 Additional Synthetic Dataset: Moons100

We report the experiments carried out on a synthetic dataset referred to as **Moons100**, which is also based on the two interleaving Moons dataset but with a different ground-truth task similarity structure. We consider a set of $K = 100$ agents, each associated with a personal rotation axis drawn from a normal distribution. We generate the local datasets by drawing a random number of points from the two Moons distribution: uniformly between 3 and 20 for training and 100 for testing. We then apply the random rotation of the agent to all its points. We further add random label noise by flipping the labels of 5% of the training data and embed all the points in \mathbb{R}^D space by adding random values for the $D - 2$ empty axes. In the experiments, the number of dimensions D is fixed to 20 and the number of base functions n to 200. For **Dada-Learned**, the graph is updated after every 200 iterations of optimizing α . We build a “ground-truth” collaboration graph where the weights between agents are computed from the angle θ_{ij} between the agents’ rotation axes, using $w_{i,j} = \exp(\frac{\cos(\theta_{ij}) - 1}{\sigma})$ with $\sigma = 0.1$. We drop all edges with negligible weights.

Figure 8 shows the evolution of the training and test accuracy over the iterations for the various approaches defined in the main text. The results are consistent with those presented for **Moons100** in the main text. They clearly show the gain in accuracy provided by our method: **Dada** is successful in reducing the overfitting of **Local-Adaboost**, and allows higher test accuracy than both **Global-Adaboost** and **Perso-linear**. Again, we see that our strategy to learn the collaboration graph can effectively make up for the absence of knowledge about the ground-truth similarities between agents. At convergence, the learned graph has an average number of neighbors per node $\mathbb{E}_k[N_k] = 42.64$, resulting in a communication complexity for

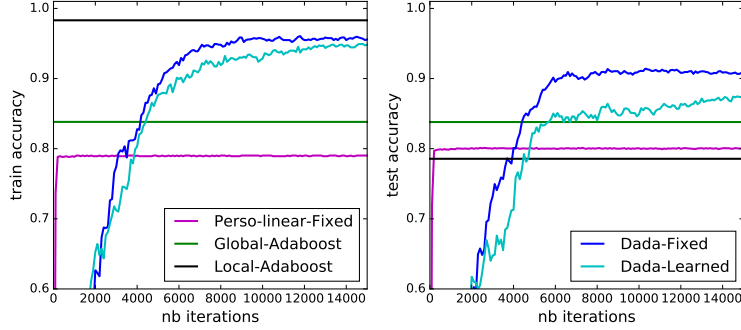


Figure 8: Training and test accuracy w.r.t. number of iterations on **Moons100**.

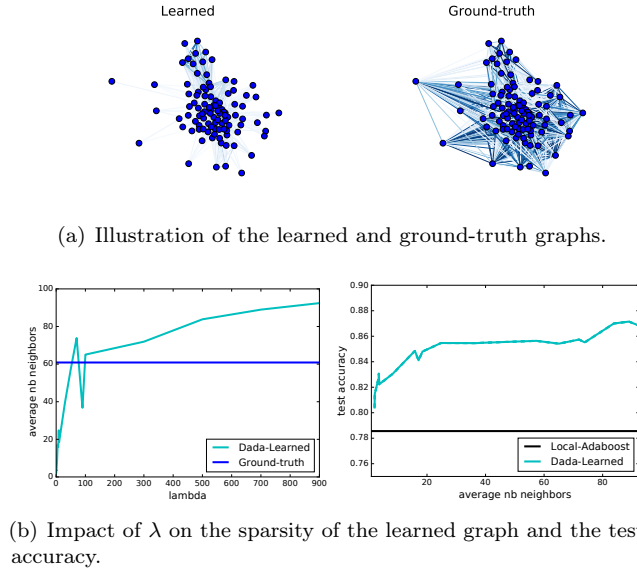


Figure 9: Graph visualization and study of the impact of graph sparsity on **Moons100**.

updating the classifiers smaller than the one of the ground-truth graph, which has $\mathbb{E}_k[|N_k|] = 60.86$ (see Figure 9). We can make the graph even more sparse (hence reducing the communication complexity of **Dada**) by setting the hyper-parameter λ to smaller values. Of course, learning a sparser graph can also a negative impact on the accuracy of the learned models. In Figure 9(b), we show this trade-off between the sparsity of the graph and the test accuracy of the models for the **Moons100** problem. As expected, as $\lambda \rightarrow 0$ the graph becomes sparser and the test accuracy tends to the performance of **Local-Adaboost**. Conversely, larger values of λ induce denser graphs, sometimes resulting in better accuracies but at the cost of higher communication complexity.

D.4 Additional Real Datasets: Computer Buyers and School

Our last set of experiments is performed on two real-world datasets used in the multi-task learning literature.

Computer Buyers⁴ consists of $K = 190$ buyers, who have each evaluated $m_k = 20$ computers described by $D = 14$ attributes, with an overall score within the range $[0, 10]$. We use a total of 1407 (between 5 and 10 per agent) instances for training and 2393 (between 10 and 15 per agent) for testing. **School** (Goldstein,

⁴<https://github.com/probml/pmtkdata/tree/master/conjointAnalysisComputerBuyers>

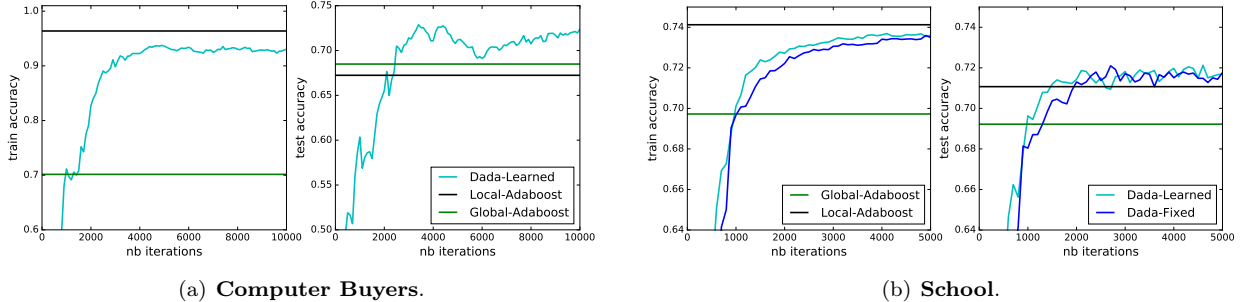


Figure 10: Training and test accuracy w.r.t. number of iterations on **Computer Buyers** and **School**. Note that no ground-truth graph is available for **Computer Buyers**.

1991)⁵ consists of $m = 15362$ total student examination records, with an overall score in the range $[0, 70]$ from $K = 140$ secondary schools. We use the $D = 17$ student features for learning the models and the remaining 11 school features (averaged over the three years of the survey) to build a pre-defined exponential graph based on the cosine similarities between school features. In total, there are 11471 instances (between 16 and 188 per agent) for training and 3889 (between 5 and 63 per agent) for testing.

We tackle both problems as binary classification tasks by affecting all instances with a score above a given threshold (5 for **Computer Buyers** and 20 for **School**) to the positive class and the remaining ones to the negative class. Finally, we set the number of base functions to $n = 28$ for **Computer Buyers** and to $n = 112$ for **School**.

In Figure 10, we plot the training and test accuracy w.r.t. the number of iterations. We see that our alternating procedure (**Dada**) converges to a better solution than those of all the competitors, which either overfit the training set or fail to capture the specificities of the local datasets. On **School**, **Dada-Learned** (learning the models and the graph) achieves results comparable to those of **Dada-Fixed** (which uses the pre-defined graph).

⁵<https://github.com/tjanez/PyMTL/tree/master/data/school>